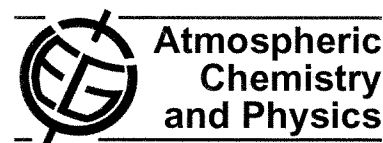


Atmos. Chem. Phys., 10, 2269–2286, 2010  
www.atmos-chem-phys.net/10/2269/2010/  
© Author(s) 2010. This work is distributed under  
the Creative Commons Attribution 3.0 License.



## Finding the missing stratospheric $\text{Br}_y$ : a global modeling study of $\text{CHBr}_3$ and $\text{CH}_2\text{Br}_2$

Q. Liang<sup>1,2,\*</sup>, R. S. Stolarski<sup>1</sup>, S. R. Kawa<sup>1</sup>, J. E. Nielsen<sup>3,4</sup>, A. R. Douglass<sup>1</sup>, J. M. Rodriguez<sup>1</sup>, D. R. Blake<sup>5</sup>, E. L. Atlas<sup>6</sup>, and L. E. Ott<sup>3,7</sup>

<sup>1</sup>NASA Goddard Space Flight Center, Atmospheric Chemistry and Dynamics Branch, Code 613.3, Greenbelt, MD 20771, USA

<sup>2</sup>Oak Ridge Associated Universities, NASA Postdoctoral Program, Oak Ridge, Tennessee 37831, USA

<sup>3</sup>NASA Goddard Space Flight Center, Global Modeling and Assimilation Office, Code 610.1, Greenbelt, MD 20771, USA

<sup>4</sup>Science Systems and Applications Inc., Lanham, Maryland, USA

<sup>5</sup>University of California, 570 Rowland Hall, Irvine, CA 92697, USA

<sup>6</sup>University of Miami, 4600 Rickenbacker Causeway, Miami, FL 33149, USA

<sup>7</sup>Goddard Earth Sciences & Technology Center, University of Maryland, Baltimore County, Maryland, USA

\* now at: Goddard Earth Sciences & Technology Center, University of Maryland, Baltimore County, Maryland, USA

Received: 2 October 2009 – Published in Atmos. Chem. Phys. Discuss.: 5 November 2009

Revised: 24 February 2010 – Accepted: 25 February 2010 – Published: 4 March 2010

**Abstract.** Recent in situ and satellite measurements suggest a contribution of  $\sim 5$  pptv to stratospheric inorganic bromine from short-lived bromocarbons. We conduct a modeling study of the two most important short-lived bromocarbons, bromoform ( $\text{CHBr}_3$ ) and dibromomethane ( $\text{CH}_2\text{Br}_2$ ), with the Goddard Earth Observing System Chemistry Climate Model (GEOS CCM) to account for this missing stratospheric bromine. We derive a “top-down” emission estimate of  $\text{CHBr}_3$  and  $\text{CH}_2\text{Br}_2$  using airborne measurements in the Pacific and North American troposphere and lower stratosphere obtained during previous NASA aircraft campaigns. Our emission estimate suggests that to reproduce the observed concentrations in the free troposphere, a global oceanic emission of  $425 \text{ Gg Br yr}^{-1}$  for  $\text{CHBr}_3$  and  $57 \text{ Gg Br yr}^{-1}$  for  $\text{CH}_2\text{Br}_2$  is needed, with 60% of emissions from open ocean and 40% from coastal regions. Although our simple emission scheme assumes no seasonal variations, the model reproduces the observed seasonal variations of the short-lived bromocarbons with high concentrations in winter and low concentrations in summer. This indicates that the seasonality of short-lived bromocarbons is largely due to seasonality in their chemical loss and transport. The inclusion

of  $\text{CHBr}_3$  and  $\text{CH}_2\text{Br}_2$  contributes  $\sim 5$  pptv bromine throughout the stratosphere. Both the source gases and inorganic bromine produced from source gas degradation ( $\text{Br}_y^{\text{VLSL}}$ ) in the troposphere are transported into the stratosphere, and are equally important. Inorganic bromine accounts for half (2.5 pptv) of the bromine from the inclusion of  $\text{CHBr}_3$  and  $\text{CH}_2\text{Br}_2$  near the tropical tropopause and its contribution rapidly increases to  $\sim 100\%$  as altitude increases. More than 85% of the wet scavenging of  $\text{Br}_y^{\text{VLSL}}$  occurs in large-scale precipitation below 500 hPa. Our sensitivity study with wet scavenging in convective updrafts switched off suggests that  $\text{Br}_y^{\text{VLSL}}$  in the stratosphere is not sensitive to convection. Convective scavenging only accounts for  $\sim 0.2$  pptv (4%) difference in inorganic bromine delivered to the stratosphere.

### 1 Introduction

Oceanic emission of very short-lived substances (VLSL) is thought to contribute significantly to reactive bromine in the stratosphere in addition to long-lived halons and methyl bromide (Kurylo and Rodriguez, 1999). VLSL are not accounted for in most chemistry climate models. In the stratosphere, inorganic bromine produced from VLSL ( $\text{Br}_y^{\text{VLSL}}$ ) contributes to catalytic destruction of ozone (e.g., McElroy et al., 1986; Solomon et al., 1995; Garcia and Solomon, 1994;



Correspondence to: Q. Liang  
([qing.liang@nasa.gov](mailto:qing.liang@nasa.gov))

Sturges et al., 2000). Br<sub>y</sub><sup>VLS</sup> can also have a significant impact on tropospheric ozone (von Glasow et al., 2004; Yang et al., 2005).

A key question is the extent to which VLS contribute to inorganic bromine (Br<sub>y</sub>) in the stratosphere. The difference between ground-based observations of column BrO (Sinnhuber et al., 2002, and references therein) and the fraction of the BrO column which can be accounted for based on long-lived halons and methyl bromide suggests a contribution of ~5 pptv to stratospheric inorganic bromine from VLS (Sinnhuber et al., 2002). This is consistent with recent balloon-borne measurements which estimated that Br<sub>y</sub><sup>VLS</sup> is ~5.2 pptv (Dorf et al., 2008). Estimates of Br<sub>y</sub><sup>VLS</sup> implied from satellite BrO measurements are more variable, ranging from ~3 pptv (Sinnhuber et al., 2005; Livesey et al., 2006) to ~8 pptv (Sioris et al., 2006). The estimated contribution of VLS to Br<sub>y</sub> in the stratosphere from modeling studies are in general significantly lower than that suggested by in situ and satellite observations. Earlier studies by Dvortsov et al. (1999) and Nielsen and Douglass (2001) calculated a maximum of 1.8 pptv and 1.1 pptv Br<sub>y</sub>, respectively, in the stratosphere from bromoform (CHBr<sub>3</sub>). More recent modeling studies by Kerkweg et al. (2008), Gettelman et al. (2009), Aschmann et al. (2009) and Hossaini et al. (2010) suggested that CHBr<sub>3</sub> and CH<sub>2</sub>Br<sub>2</sub> contribute significant amounts of reactive bromine to the lower stratosphere, with the calculated contribution varying between ~2–3 pptv among individual studies. One exception is the modeling study by Warwick et al. (2006) which presented a detailed emission-based modeling analysis of all five major VSL oceanic bromocarbons, including CHBr<sub>3</sub>, dibromomethane (CH<sub>2</sub>Br<sub>2</sub>), bromodichloromethane (CHBrCl<sub>2</sub>), dibromochloromethane (CHBr<sub>2</sub>Cl), and bromochloromethane (CH<sub>2</sub>BrCl). They concluded that very short-lived (VSL) oceanic bromocarbons contribute a maximum of 6–7 pptv Br<sub>y</sub>, peaking over the equator at ~100 hPa.

A large part of the uncertainty in the contribution of VLS to Br<sub>y</sub> in the stratosphere arises from the highly-variable mixing ratios of VSL bromocarbons in the marine boundary layer, ranging from 0.2 pptv to >100 pptv (Quack and Wallace, 2003). Therefore, the amount of VSL bromocarbons that enters the free troposphere and stratosphere and its subsequent inorganic bromine may vary depending on the location and timing of emissions. The current estimate of the oceanic emissions of VSL bromocarbons is highly uncertain. Bottom-up emission estimates based on atmospheric and oceanic surface water observations indicate that sea-to-air flux of CHBr<sub>3</sub> is between 210–820 Gg Br yr<sup>-1</sup> (Carpenter and Liss, 2000; Quack and Wallace, 2003; Yokouchi et al., 2005; Butler et al., 2007) and that for CH<sub>2</sub>Br<sub>2</sub> ranges between 61–280 Gg Br yr<sup>-1</sup> (Yokouchi et al., 2005; Butler et al., 2007). Modeling studies that derive top-down emission estimates by reproducing background atmospheric concentrations suggest that global emission of CHBr<sub>3</sub> ranges

between 190–570 Gg Br yr<sup>-1</sup> (e.g. Dvortsov et al., 1999; Kurylo and Rodriguez, 1999; Nielsen and Douglass, 2001; Warwick et al., 2006) and that of CH<sub>2</sub>Br<sub>2</sub> is between 43–104 Gg Br yr<sup>-1</sup> (e.g. Dvortsov et al., 1999; Warwick et al., 2006).

Another important contributor to the uncertainty is related to the transport and dehydration process in the tropical tropopause layer (TTL). Convective lofting is suggested to be the most important pathway of air entering the stratosphere (e.g. Sinnhuber and Folkins, 2006; Fueglistaler et al., 2009). Air masses entering the stratosphere must be dehydrated and soluble substances, e.g. Br<sub>y</sub>, carried within these air masses are subject to wet scavenging during troposphere-to-stratosphere transport. The process of dehydration is not well understood. Past studies suggest that dehydration can occur slowly by falling ice during slow ascent through the TTL (Holton and Gettelman, 2001; Fueglistaler et al., 2005) or more rapidly in deep convective overshooting (Sherwood and Dessler, 2000). As a result, the rate of wet scavenging of Br<sub>y</sub>, which depends on the mechanism of dehydration, is highly uncertain. Model sensitivity studies suggest that the contribution of CHBr<sub>3</sub> to stratospheric bromine range from 0.5–1.6 pptv when Br<sub>y</sub> is removed completely in convective updraft to ~3 pptv assuming no washout (Sinnhuber and Folkins, 2005; Aschmann et al., 2009).

In this paper, we use the GEOS Chemistry Climate Model (GEOS CCM) together with aircraft measurements from previous NASA field missions to derive a top-down emission estimate of CHBr<sub>3</sub> and CH<sub>2</sub>Br<sub>2</sub>, the two most important VSL bromocarbons. Together, CHBr<sub>3</sub> and CH<sub>2</sub>Br<sub>2</sub> account for >80% VSL organic bromine in the marine boundary layer and free troposphere (WMO, 2007). We present a quantitative estimate of their contribution to reactive bromine in the stratosphere with our optimized emission. Compared to many previous studies, this study has two major improvements. First, we derive the top-down emission estimate and evaluate model results with an extensive set of aircraft measurements obtained during eight previous NASA field missions throughout the Pacific/North America region. The broad spatial and temporal coverage of these measurements lends more confidence in the robustness of our derived results. Secondly, unlike many previous modeling studies that assume a constant wash-out lifetime of Br<sub>y</sub> (10-days in Dvortsov et al., 1999, Nielsen and Douglass, 2001; Warwick et al., 2006; Hossaini et al., 2010; 0 to indefinite days in Sinnhuber and Folkins, 2005) or a relative simple washout process (Aschmann et al., 2009), we implement a detailed wet deposition scheme that includes scavenging in convective updrafts and rainout/washout in large-scale precipitation. This is to assure a more realistic representation of the impact of large-scale/convective transport on the highly soluble Br<sub>y</sub>.

## 2 Model

### 2.1 Description

Model simulations are conducted using the Goddard Space Flight Center (GSFC) GEOS CCM Version 2 (V2), an augmented version of GEOS CCM Version 1 (V1) as described in Pawson et al. (2008). The model has a spatial resolution of 2° latitude by 2.5° longitude and 72 layers extending from the surface to 0.01 hPa. The model couples the GEOS-5 GCM (Reinecker et al., 2008) with an updated version of the stratospheric chemistry module described by Douglass and Kawa (1999). The photochemical scheme includes all important gas phase reactions for the stratosphere (Douglass and Kawa, 1999) and uses the chemical kinetics from JPL 2006. Photolysis rates are calculated using the temperature dependent cross sections from JPL 2006. The model uses a flux-form semi-Lagrangian dynamical core (Lin, 2004). Moist processes in GEOS-5 are represented using a convective parameterization and prognostic cloud scheme. Convection is parameterized using the relaxed Arakawa Schubert (RAS) scheme developed by Moorthi and Suarez (1992) in which the atmosphere is relaxed towards equilibrium. Ott et al. (2010) provides a detailed analysis of the GEOS-5 moist physics scheme and its impact on tracer transport, describing the prognostic cloud scheme and comparing results with observations. The scheme calculates large-scale ice and liquid condensate by assuming a probability distribution function for total water. Condensate is subsequently removed from the model domain by evaporation, auto-conversion of liquid condensate, sedimentation of frozen condensate, and accretion of condensate by falling precipitation. The GEOS-5 GCM produces general precipitation patterns that correlate well with the Global Precipitation Climatology Project (GPCP) data ( $r = 0.65$ ). The stratospheric and tropospheric transport produced by the GEOS-CCM has been extensively evaluated in many previous studies (e.g. Eyring et al., 2006; Waugh et al., 2007; Pawson et al., 2008; Douglass et al., 2008; Liang et al., 2008). The GEOS CCM simulations agree well with observations in many of the meteorological, transport-related, and chemical diagnostics. Of particular relevance to this study, Douglass et al. (2008) and Waugh et al. (2007) show that the GEOS CCM reproduces well the mean atmospheric circulation with realistic age-of-air, and therefore a realistic representation of the troposphere-to-stratosphere and the subsequent transport.

### 2.2 Bromine chemistry in the GEOS CCM

For this study, we modify the standard stratospheric photochemistry scheme to include simple VSL bromocarbon chemistry. In this simple chemistry scheme, CHBr<sub>3</sub> and CH<sub>2</sub>Br<sub>2</sub> are destroyed via photolysis and reaction with OH. Photolysis rates are calculated using the JPL 2006 cross sections. Rates of reaction with OH are calculated using

temperature-dependent expressions from JPL 2006. OH above the tropopause is calculated online in the stratospheric chemistry module. Below the tropopause, OH is relaxed to zonal-averaged 2-dimensional monthly mean fields archived during a full chemistry simulation from the GEOS-Chem chemistry transport model (Bey et al., 2001). GEOS-Chem includes detailed tropospheric O<sub>3</sub>-NO<sub>x</sub>-NMHC chemistry and the simulated OH compares reasonably well with observations (Bey et al., 2001). The mean tropospheric OH concentration is  $11 \times 10^5$  molecules cm<sup>-3</sup> and yields an atmospheric lifetime of 5.1 years for methyl chloroform, within the uncertainty of observational estimates (Bey et al., 2001).

Since >80% of the inorganic bromine produced by the degradation of CHBr<sub>3</sub> and CH<sub>2</sub>Br<sub>2</sub> (Br<sub>y</sub><sup>VSL</sup>) in the troposphere is in the form of hydrobromic acid (HBr) and hypobromous acid (HOBr) and both are highly soluble (Yang et al., 2005), for simplicity, we track the degradation products as a single tracer. Br<sub>y</sub><sup>VSL</sup> is transported as an individual tracer and subject to wet and dry deposition, but does not interact with standard stratospheric chemistry. We adopt the wet and dry deposition scheme from the Goddard Chemistry Aerosol Radiation and Transport (GOCART) model (Chin et al., 2000a). Dry deposition includes gravitational settling with a uniform deposition velocity of 0.3 cm/s, a simplified value based on Yang et al. (2005). Wet deposition includes scavenging in rainout (in-cloud precipitation) and washout (below-cloud precipitation) in large-scale precipitation (Giorgi and Chameides, 1986) and in deep convective updrafts (Balkanski et al., 1993). The VSL bromocarbons are in general insoluble and not subject to wet scavenging. We assume high solubility for Br<sub>y</sub>. Washout and rainout of Br<sub>y</sub> by large-scale rain are computed as first-order processes using parameters from Giorgi and Chameides (1986) and the simulated precipitation rate. Convective scavenging occurs in the moist convection process with a scavenging efficiency of 1 km<sup>-1</sup>, equivalent to 100% removal. When evaporation occurs during large-scale and convective transport, a fraction of the dissolved Br<sub>y</sub> proportional to the evaporated water is released back to the atmosphere (Chin et al., 2000a). This wet scavenging scheme has been applied in many atmospheric modeling studies of soluble aerosols, e.g. sulfate, sea salt, dust, and the simulated concentrations compare well with surface observations at many observation sites around the globe (e.g. Chin et al., 2000b, 2007; Ginoux et al., 2001).

Figure 1 presents the calculated lifetime of CHBr<sub>3</sub> and CH<sub>2</sub>Br<sub>2</sub> from the GEOS CCM bromocarbon simulation. Local lifetime of VSL bromocarbons varies significantly from ~15 days for CHBr<sub>3</sub> and ~90 days for CH<sub>2</sub>Br<sub>2</sub> in the tropics to ~180 days (CHBr<sub>3</sub>) and ~540 days (CH<sub>2</sub>Br<sub>2</sub>) in the poles, similar to the results in Dvortsov et al. (1999) and Hossaini et al. (2010). Dvortsov et al. (1999) calculated that the tropical tropospheric lifetime of CHBr<sub>3</sub> is of the order of 2–3 weeks and that of CH<sub>2</sub>Br<sub>2</sub> is 2–3 months. Hossaini et al. (2010) showed that local lifetime of CHBr<sub>3</sub> ranges between ~15 days (compared to ~13 days in this work) at

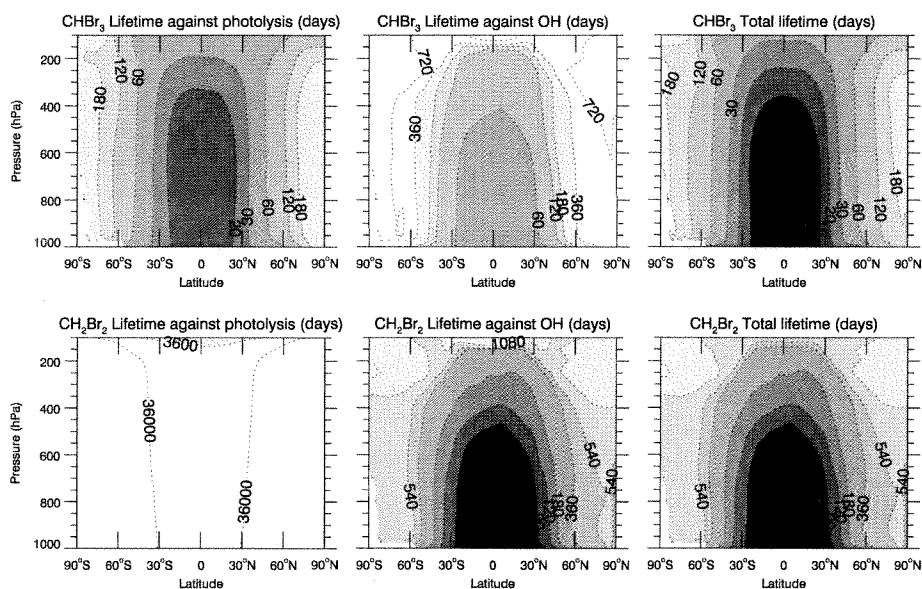


**Fig. 1.** Model calculated local lifetime of CHBr<sub>3</sub> and CH<sub>2</sub>Br<sub>2</sub> against photolysis, reaction with OH, and total lifetime.

the tropical surface to ~25–30 days (30 days this work) in the TTL, and that of CH<sub>2</sub>Br<sub>2</sub> ranges from ~50 days (~70 days this work) at the surface to ~520 days (~540 days this work) in the TTL. Though local lifetime of VSL bromocarbons is highly variable, the global-integrated atmospheric lifetime is heavily weighted by loss in the tropical lower atmosphere where emissions are high and degradation occurs rapidly. The global-integrated atmospheric lifetime ( $\tau$ ) of CHBr<sub>3</sub> is 20 days (annual average) in our simulation with photolysis being the dominant sink ( $\tau_{hv}$ =27 days,  $\tau_{OH}$ =81 days), consistent with the lifetime calculated in Warwick et al. (2006) (varying between 15–37 days with the choice of emissions) and Kerkweg et al. (2008) (20 days). Degradation of CH<sub>2</sub>Br<sub>2</sub> occurs predominantly via reaction with OH ( $\tau_{hv}$ =8300 days,  $\tau_{OH}$ =143 days). The simulated atmospheric lifetime of CH<sub>2</sub>Br<sub>2</sub> is 140 days, longer than the 100 days calculated in Kerkweg et al. (2008). Our simulated seasonal cycle of CHBr<sub>3</sub> at Hawaii (maximum in winter ~0.7 pptv and minimum in summer ~0.3 pptv) matches well with observations from Atlas and Ridley (1996). This seasonal cycle is generated by transport and chemistry in the lower troposphere (Nielsen and Douglass, 2001), which implies that the model captures well chemical loss and tropospheric transport processes.

The simulated atmospheric lifetime of Br<sub>y</sub><sup>VLSL</sup> against wet deposition is ~15 days with column-integrated rainout/washout lifetime varying from ~10 days in the tropics to ~2 months at high latitudes. The calculated lifetime of Br<sub>y</sub><sup>VLSL</sup> against dry deposition is greater than 20 years, suggesting surface dry deposition is of negligible importance compared with wet scavenging.

### 3 Emission scenarios

In this work, we derive a “top-down” emission scenario (Scenario A) of CHBr<sub>3</sub> and CH<sub>2</sub>Br<sub>2</sub> using observations from previous aircraft campaigns as constraints. We conduct a 12-year GEOS CCM bromine simulation with emission Scenario A and examine the chemistry and transport of VSL bromocarbons and their degradation product, Br<sub>y</sub><sup>VLSL</sup>, in the atmosphere. The simulation is driven by sea surface temperatures (SST) from 1990 to 2001, but otherwise does not correspond to any specific year. We initialized the simulation with zero-concentrations for CHBr<sub>3</sub> and CH<sub>2</sub>Br<sub>2</sub>. For CHBr<sub>3</sub> (lifetime ~1 month) and CH<sub>2</sub>Br<sub>2</sub> (lifetime of ~4 months) a 3 year simulation length has been used by most previous modeling studies and is generally thought to be adequate. However, transport in the stratosphere is slow and Br<sub>y</sub> has no significant loss process in the atmosphere other than removal by wet scavenging in the troposphere, thus a 3 year simulation is not sufficient to quantitatively understand the contribution of VSL bromocarbons to reactive bromine in the stratosphere. Here we extend the simulation length to 12 years to investigate whether the duration of simulation affects the troposphere-to-stratosphere transport of Br<sub>y</sub>.

We conduct two sensitivity simulations with two additional emission scenarios (Scenario B and C) from Warwick et al. (2006), which were demonstrated to reproduce well the observed CHBr<sub>3</sub> concentrations during the NASA PEM-Tropics mission. For computational efficiency, the two sensitivity simulations are run for three years driven by SST from 1990–1992. Results from year 3 from all three simulations are compared with each other to understand the impact of

**Table 1.** Emission distribution of CHBr<sub>3</sub> and CH<sub>2</sub>Br<sub>2</sub> in Scenario A, B and C.

Global emissions Gg Br yr <sup>-1</sup>	Emission distribution						
	CHBr <sub>3</sub> (CH <sub>2</sub> Br <sub>2</sub> ) <sup>a</sup>	Latitude	Open ocean Percentage	Gg Br yr <sup>-1a</sup>	Latitude	Coast Percentage	Gg Br yr <sup>-1a</sup>
Scenario A	425 (57)	5–90° S	1.1%	5 (1)	50–90° S	1.1%	5 (1)
		10–50° S	11.1%	47 (6)	10–50° S	11.1%	47 (6)
		10° S–10° N	33.3%	141 (20)	10° S–10° N	4.4%	19 (3)
		10–50° N	13.3%	57 (8)	10–50° N	22.2%	94 (13)
		50–90° N	1.1%	5 (1)	50–90° N	1.1%	5 (1)
Scenario B	380 (104)	20° S–20° N	75%	285 (78)	None		
		20–50° S/N	25%	95 (26)			
Scenario C	565 (57)	20° S–20° N	37.8%	214 (21)	10° S–10° N	49.6%	280 (29)
		20–50° S/N	6.3%	71 (7)			

<sup>a</sup> Emissions of CH<sub>2</sub>Br<sub>2</sub> are in the parentheses.

emission distribution on simulated bromocarbon concentrations.

The details of each scenario are listed in Table 1 and emission distributions are presented in Fig. 2. For simplicity we assume no seasonal variability in emissions in all three scenarios. We refer to the three simulations as simulation A (with emission Scenario A), simulation B (with Scenario B), and simulation C (with Scenario C).

### 3.1 Scenario A

We use measurements from eight NASA aircraft missions between 1996 and 2008 as observational constraints. A detailed list of the aircraft missions is presented in Table 2 and the geographic distribution of all flight tracks is shown in Fig. 3. The composite of bromocarbon measurements in the troposphere covers the entire Pacific and North America region. Measurements in the upper troposphere/lower stratosphere (UT/LS) are concentrated in the tropics. Whole air samples were collected by stainless steel canisters onboard the NASA DC-8, ER-2, and WB-57F aircrafts and later analyzed using gas chromatography with mass selective detection (GC/MS) (Schauffler et al., 1999; Blake et al., 2003).

We derive the emission distribution of CHBr<sub>3</sub> following a similar approach as that introduced in Warwick et al. (2006) and use Scenario 5 of Warwick et al. (2006) (Scenario C below) as our baseline emission. We use 10 individual components to represent emissions from open ocean and coastlines near the equatorial tropics, and at the mid and high latitudes, respectively. Multiple sensitivity runs are conducted by varying the magnitude of emission for each region and the latitudinal border of each region. The optimum emission estimate for each region is determined by simultaneously matching i) the observed concentration in the middle troposphere and ii) the observed vertical gradient in the corresponding

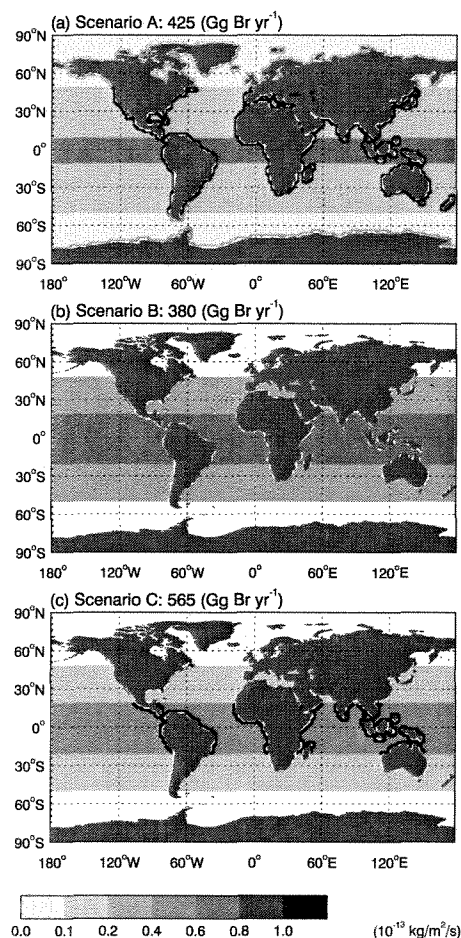


**Fig. 2.** Global emission distribution of CHBr<sub>3</sub> for (a) Scenario A, (b) Scenario B, and (c) Scenario C.

**Table 2.** A summary of aircraft observations used in this study.

Missions		Time	Area	References
PEM-Tropics <sup>1</sup>	PEM-Tropics A	August–October 1996	75° S–50° N, 150° E–100° W	Hoell et al. (1999)
	PEM-Tropics B	March–April 1999	40° S–40° N, 140° E–70° W	Raper et al. (2001)
TRACE-P <sup>2</sup>		February–April 2001	10–40° N, 140° E–80° W	Jacob et al. (2003)
INTEX <sup>3</sup>	INTEX-A	July–August 2004	10–45° N, 70–130° W	Singh et al. (2006)
	INTEX-B	March–May 2006	15–70° N, 170° E–90° W	Singh et al. (2009)
TC4 <sup>4</sup>		July–August 2007	10° S–40° N, 60–130° W	Toon et al. (2010)
ARCTAS <sup>5</sup>	ARCTAS-A	April 2008	30–90° N, 20° E–50° W	Jacob et al. (2009)
	ARCTAS-B	June–July 2008	30–90° N, 20–140° W	Jacob et al. (2009)
STRAT <sup>6</sup>		January–December 1996	5° S–65° N, 80–160° W	Schauffler et al. (1999)
Pre-AVE <sup>7</sup>		January–February 2004	10° S–40° N, 80–100° W	
AVE <sup>8</sup>	HAVE-2	June 2005	15–50° N, 70–100° W	Kroon et al. (2008)
	CRAVE	January–February 2006	0–40° N, 80–100° W	Kroon et al. (2008)

<sup>1</sup> The Pacific Exploratory Missions – Tropics (PEM-Tropics) mission.

<sup>2</sup> The Transport and Chemical Evolution over the Pacific (TRACE-P) mission.

<sup>3</sup> The Intercontinental Chemical Transport Experiment (INTEX) mission.

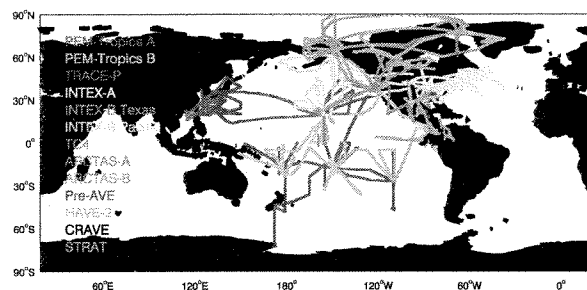
<sup>4</sup> The Tropical Composition, Cloud and Climate Coupling (TC4) mission.

<sup>5</sup> The Arctic Research of the Composition of the Troposphere from Aircraft and Satellites (ARCTAS) mission.

<sup>6</sup> The Stratospheric Tracers of Atmospheric Transport (STRAT) mission.

<sup>7</sup> The Pre-Aura Validation Experiment (Pre-AVE).

<sup>8</sup> The Aura Validation Experiment (AVE). Data from two AVE campaigns are used in this study: i) 2005 June Houston AVE (HAVE-2) campaign, ii) 2006 January Costa Rica AVE (CRAVE) campaign.

**Fig. 3.** Flight tracks for all aircraft missions used in this study (Table 2).

region. Measured concentrations of CHBr<sub>3</sub> and CH<sub>2</sub>Br<sub>2</sub> in the coastal marine boundary layer are highly correlated (Yokouchi et al., 2005), suggesting they are produced by similar marine macroalgae sources and therefore have similar source distributions (Carpenter et al., 1999). Atmospheric measurements from the aircraft campaigns used in this study also show consistent high correlations (correlation coefficients range between 0.59 and 0.96 for individual missions) between the measured concentrations of CHBr<sub>3</sub> and CH<sub>2</sub>Br<sub>2</sub> below 1 km altitude. Therefore, we employ the same distri-

bution for CH<sub>2</sub>Br<sub>2</sub> as that derived for CHBr<sub>3</sub>. The global emission magnitude for CH<sub>2</sub>Br<sub>2</sub> is deduced by matching the simulated concentrations with background atmospheric observations. To avoid redundancy, we present here only the optimum emission estimate (Scenario A).

In our optimum emission estimate, we separate global emissions into 10 individual components representing emissions from open ocean and coastlines at 10° S–10° N, 10–50° S/° N, and 50–90° S/° N, respectively (Fig. 2 and Table 1). Our best estimate yields a global emission of 425 Gg Br yr<sup>-1</sup> for CHBr<sub>3</sub>, with 255 Gg Br yr<sup>-1</sup> (60%) and 170 Gg Br yr<sup>-1</sup> (40%) over the open ocean and along the coastlines, respectively. Our estimate of CHBr<sub>3</sub> emission from coastal regions is similar to the bottom-up coastal estimate of 200 Gg Br yr<sup>-1</sup> from Carpenter et al. (2009). The emission is latitude-dependent, with 160 Gg Br yr<sup>-1</sup> (~38%) concentrated in a narrow tropical band between 10° S and 10° N, 95 Gg Br yr<sup>-1</sup> (22%) and 150 Gg Br yr<sup>-1</sup> (35%) in the Southern and Northern sub-tropics and mid-latitudes between 10° and 50° north and south, respectively. A small amount, 10 Gg Br yr<sup>-1</sup>, is emitted at the Northern and Southern high latitudes, respectively. The global emission of CH<sub>2</sub>Br<sub>2</sub> is estimated to be 57 Gg Br yr<sup>-1</sup>. Note that we derive our emission estimates using the background concentration as an observational constraint. In general, global chemistry models,

even with top-down emission estimate, tend to miss the influence of strongly localized sources (with concentrations much higher than background concentrations), e.g. along coasts and edges of ice sheets. As a result, our global emission estimate of the oceanic emission for VSL bromocarbons and the percentage of coastal emissions (40%) are likely a low limit estimate (Quack and Wallace, 2003). The localized sources are confined to regions much smaller than a typical model grid box (2° latitude by 2.5° longitude in this study). If the model were to fill the entire grid box with emissions large enough to reproduce the observed localized high concentrations, the simulated concentrations in the background atmosphere would be too high compared with observations.

### 3.2 Scenario B

This scenario uses the emission distribution of Scenario 3 from Warwick et al. (2006). In this scenario, a total of 380 Gg Br yr<sup>-1</sup> for CHBr<sub>3</sub> and 104 Gg Br yr<sup>-1</sup> for CH<sub>2</sub>Br<sub>2</sub> are emitted at the surface. The emissions are concentrated in the tropical open oceans, with 75% distributed uniformly in the open ocean between 20° S and 20° N and the remaining 25% between 20° and 50° north and south (Fig. 2 and Table 1).

### 3.3 Scenario C

This is based on Scenario 5 of Warwick et al. (2006). We follow Warwick et al. (2006) and use a global emission of 565 Gg Br yr<sup>-1</sup> for CHBr<sub>3</sub>. We reduce the global emission of CH<sub>2</sub>Br<sub>2</sub> to 57 Gg Br yr<sup>-1</sup> to correct the model high bias as compared to observations (Sect. 4). The emission distribution contains a combination of open ocean emissions and tropical coastline emissions, with ~50% emitted in the open ocean between 50° S and 50° N, and the remaining 50% along the tropical coastline between 10° S and 10° N (Fig. 2 and Table 1).

## 4 Comparison with observations

### 4.1 CHBr<sub>3</sub>

We compare the simulated bromocarbons with the composite of aircraft measurements. Figure 4 shows the observed and simulated CHBr<sub>3</sub> concentrations in the lower troposphere between 800–1000 hPa. We separate aircraft observations into two periods, February–May and June–October, which approximate the boreal spring and summer seasons, respectively. Since more than 95% of the observations are made between March–May (MAM) and July–September (JAS), we compare the spring and summer observations with the simulated mean MAM and JAS CHBr<sub>3</sub> concentrations, respectively. Both the observed and simulated CHBr<sub>3</sub> are regridded to a horizontal resolution of 10° × 8° for easy comparison. In addition, we have added two panels (Fig. 4, middle column)

showing simulated CHBr<sub>3</sub> at locations where there are observations available for clear side-by-side comparison.

High CHBr<sub>3</sub> concentrations are found in a narrow tropical band between 10° S–10° N as well as along the coasts, in contrast to relatively low values in the northern/southern central Pacific and the center of the continents. This spatial distribution is consistent with the short atmospheric lifetime of CHBr<sub>3</sub>. As a result, high concentrations of CHBr<sub>3</sub> are found only in close proximity to the source regions. CHBr<sub>3</sub> also shows significant seasonal contrast in concentrations with high values during cold seasons and low values during warm seasons. Despite a simple emission scheme with no seasonality, the model reproduces well the spatial distribution and seasonal variation of CHBr<sub>3</sub>. The simulated CHBr<sub>3</sub> correlates well with the observations ( $r = 0.63$ ). This indicates the seasonal variability of CHBr<sub>3</sub> is largely controlled by the seasonality in chemical loss and tropospheric transport (Nielsen and Douglass, 2001). The lower concentrations during warm seasons are due to efficient chemical destruction by photolysis and reaction with OH. High emission near the equator (between 10° S–10° N) is likely associated with tropical upwelling and active planktonic production, as previously observed in the equatorial Pacific (Atlas et al., 1993) and the tropical East Atlantic Ocean (Class et al., 1986). Sensitivity simulations show that confining the high open ocean emission between 10° S–10° N is essential in re-creating the high concentration band in the tropics. This is due to the near-zonal advection in the equatorial Pacific associated with surface trade winds. If the high emission band were extended further, an abrupt increase in photolysis rates or OH concentration from 10° S–10° N to 10–20° S/N would be needed to reproduce the contrast in the observed CHBr<sub>3</sub> mixing ratios between 10° S–10° N and 10–20° S/N, which is unphysical. Narrowing the high emission band to 5° S–5° N, on the other band, would have led to a high concentration band too narrow compared to the observations when results are plotted at 2.5° × 2° resolution (not shown). The very high VSL bromocarbons observed in the eastern tropical Atlantic (Class et al., 1986; Quack et al., 2004 and 2007; Carpenter et al. 2009) appear to be a local phenomena. Butler et al. (2007) find no evidence for a tropical maxima in CHBr<sub>3</sub> over the open Atlantic. We conduct a sensitivity simulation with no tropical (between 10° N–10° S) emission maxima in the Atlantic to understand how this affects the global emission estimate and Br<sub>y</sub><sup>VSL</sup>. The resulted global emission decreases by 1.6% to 418 Gg Br yr<sup>-1</sup> for CHBr<sub>3</sub> and 55 Gg Br yr<sup>-1</sup> for CH<sub>2</sub>Br<sub>2</sub>. The impact on total bromine in the lower stratosphere is also small, ~0.12 pptv.

Figure 5 shows the latitudinal dependence of CHBr<sub>3</sub> at the surface. We average aircraft measurements between 0–1 km for every 10° latitude band. Surface CHBr<sub>3</sub> maximizes in the tropics as well as the high latitudes. Minimum CHBr<sub>3</sub> concentrations are found at ~30° S/N. The peak in the tropics is due to high emissions while the peaks at the high latitudes

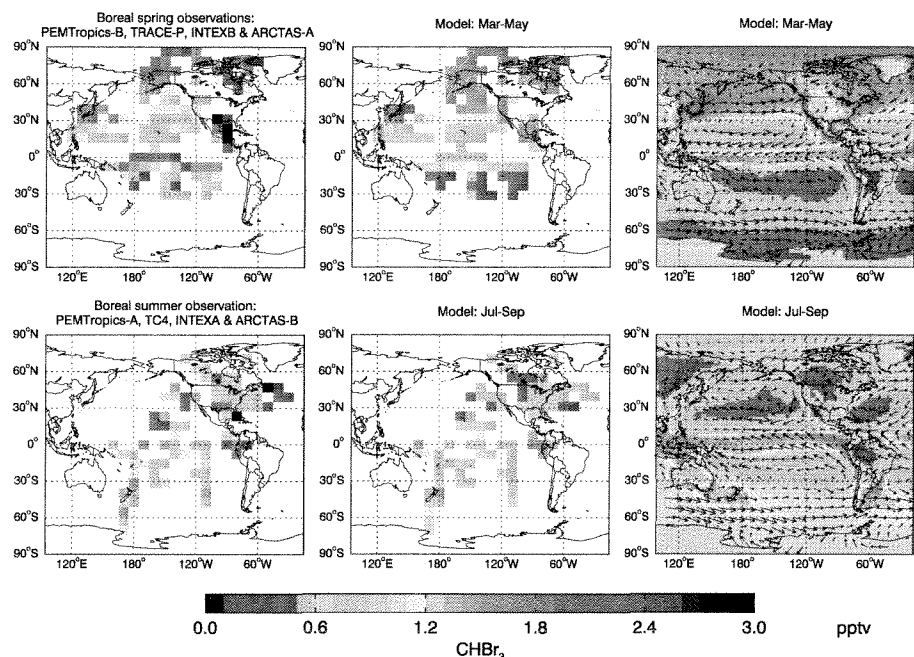


**Fig. 4.** Left column: the composite of airborne observations of  $\text{CHBr}_3$  in the lower troposphere (1000–800 hPa) during boreal spring and summer. Middle column: the simulated 1000–800 hPa mean  $\text{CHBr}_3$  between March–May (upper panel) and July–September (lower panel), sampled at the same location as the observations. Right column: same as the middle column but for the entire Pacific/North American region. The model results are from the simulation run with emission Scenario A.

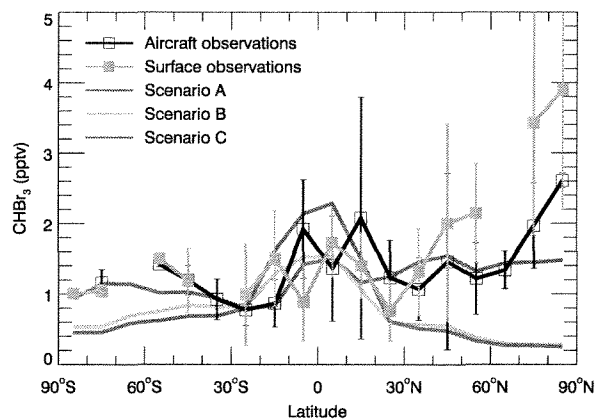


**Fig. 5.** Latitudinal dependence of  $\text{CHBr}_3$  at the surface. Black line (open squares indicate mean and vertical bar indicate one standard deviation) shows aircraft observations averaged below 1 km for each  $10^\circ$  latitude band. Surface measurements from Table 2 in Quack and Wallace (2003) are plotted in gray line with filled squares. The simulated zonal averaged  $\text{CHBr}_3$  between 0–1 km are plotted in color. We use consistent colored lines for model results from different simulations for this figure, Figs. 6, 7, 9, and 10: simulations with emission Scenario A in red, Scenario B in green, and Scenario C in blue.

are the result of relatively long lifetime. This latitudinal variation agrees well with that from previous surface measurements listed in Table 2 in Quack and Wallace (2003), which includes all published atmospheric mixing ratios of  $\text{CHBr}_3$  prior to 2003. The model reproduces relatively well the latitudinal dependence of  $\text{CHBr}_3$  except an underestimate of  $\sim 1$  pptv in the Arctic. This model-observation difference is likely a result of under-representation of emission at the ice-water interface, associated with emission from ice algae (Sturges et al., 1992, 1997), which is difficult to reproduce with a coarse model resolution.

We further compare the simulated vertical profiles of  $\text{CHBr}_3$  with observations for individual aircraft missions (Fig. 6). We sample the model at the nearest grid point to the measurement location in the corresponding month. Mixing ratio of  $\text{CHBr}_3$  at the surface is  $\sim 1$ – $2$  pptv, and decreases rapidly to  $\sim 0.6$  pptv in the middle troposphere and to  $< 0.4$  pptv near 200 hPa. Although regions covered by individual aircraft missions differ greatly from each other and we deploy a simplified zonal-uniform emission scheme, the model in general reproduces reasonably well the observed concentration, variability, and vertical gradient during most of the missions. The overestimate during ARCTAS-A is most likely due to the lack of seasonality in our oceanic emission of VSL bromocarbons. To match both the observed profile from ARCTAS-A (April) and ARCTAS-B (July) would



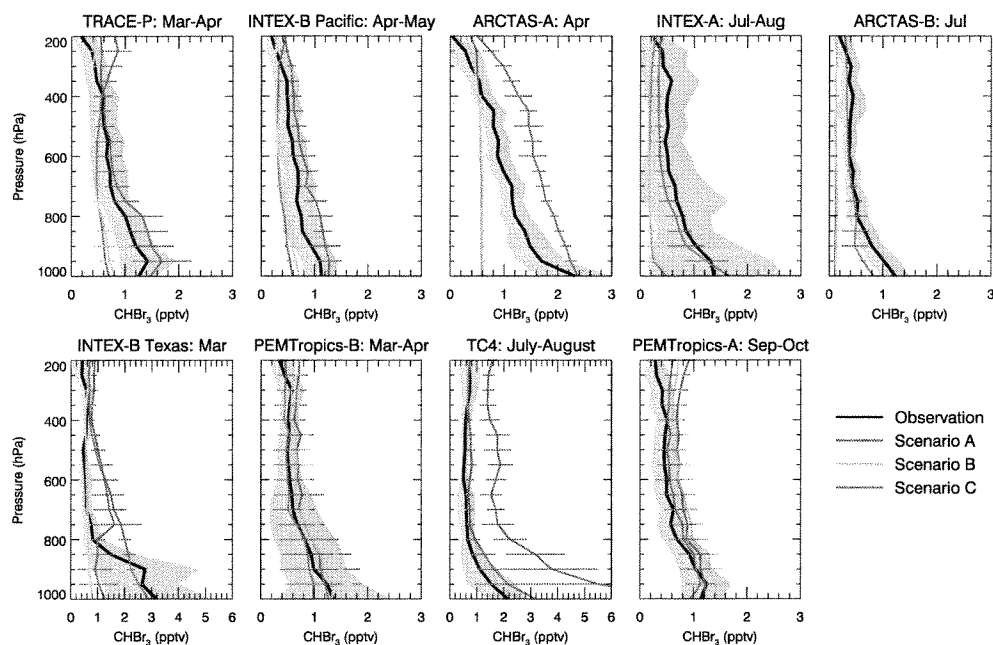


**Fig. 6.** Comparison of the observed and simulated vertical profiles of CHBr<sub>3</sub> in the troposphere during individual aircraft missions. The upper row shows missions that took place in the northern mid and high latitudes and the lower row shows those in the tropics and southern hemisphere. Black lines show the observed mean concentrations with one standard deviation marked by gray shading. The mean CH<sub>2</sub>Br<sub>2</sub> vertical profiles from three simulations are plotted in color with horizontal bars indicate one standard deviation. Model is sampled at the same location as the observations in the corresponding month.

require a seasonal-varying emission in the high latitudes with about zero emission in winter and a peak in summer. This seasonality agrees well with several previous studies, suggesting that CHBr<sub>3</sub> released from macroalgae maximizes in summer due to enhanced tissue decay and light stimulation (e.g. Goodwin et al., 1997; Klick et al. 1993; Carpenter et al., 2000).

The model does not capture the vertical gradient or variability of CHBr<sub>3</sub> observed during the INTEX-B Texas deployment. Significant forest fire plumes were sampled during INTEX-B (Singh et al., 2009). A close examination of trace gas measurements along flight tracks shows that high CHBr<sub>3</sub> mixing ratios are coincident with high levels of tracers for biomass burning, e.g. carbon monoxide, hydrogen cyanide and acetonitrile. This suggests that biomass burning is a possible additional source of CHBr<sub>3</sub>. High mixing ratios of CHBr<sub>3</sub> associated with African savannah biomass burning plumes were documented in Carpenter et al. (2007). The lack of biomass burning emissions can also explain the lack of variability in simulated CHBr<sub>3</sub> mixing ratios compared with the high variability observed in the INTEX-A mission, during which significant biomass burning plumes were sampled (Turquety et al., 2007; Liang et al., 2007).

Observed CHBr<sub>3</sub> mixing ratios in the UT/LS during recent missions, Pre-AVE, AVE, and TC4 (0.2–0.3 pptv), are significantly higher than that measured during the early STRAT mission (<0.1 pptv) (Fig. 7). This is intriguing since long-term observations at the surface display little interannual variability in CHBr<sub>3</sub> concentrations (WMO, 2007). The GEOS CCM reproduces well the observed CHBr<sub>3</sub> concentrations in the UT/LS when compared against measurements obtained during Pre-AVE, AVE, and TC4 field missions (Fig. 7), suggesting a good representation of the atmospheric losses and troposphere-to-stratosphere transport of CHBr<sub>3</sub> in the UT/LS in the GEOS CCM. The model fails to produce the very low concentrations observed during STRAT between 80–200 hPa. A similar problem was identified by Dvortsov et al. (1999) and Nielsen and Douglass (2001). Both attribute this model-observation difference to excessive convective transport from the boundary layer to the upper troposphere. The fact that GEOS CCM captures well the observed profiles during Pre-AVE, AVE, and TC4 implies that the overestimate during STRAT may not be due to excessive convective transport. The difference between the CHBr<sub>3</sub> during STRAT and that during Pre-AVE has been previously noted in Sinnhuber and Folkins (2006) and was suggested to reflect the differences in the activity of deep convection between the missions. We have examined in detail

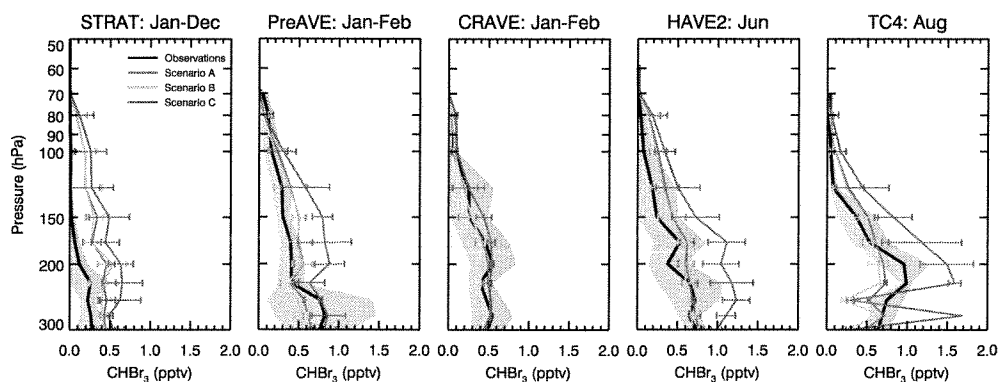


Fig. 7. Similar to figure 6 but for the UT/LS region.

the location of measurements and how the canister samples were processed during STRAT. We conclude that the difference is likely due to two reasons. First the difference is possibly due to the natural variability of short-lived species in the upper troposphere and their relationship to recent or past convection. The spatial domain of the STRAT measurements between 80–200 hPa (where there are significant differences between observations and simulated concentrations) is much smaller compared to the other missions. Measurements from the Pre-AVE, AVE, and TC4 missions indicate that there is significant spatial variability in the observed concentrations of CHBr<sub>3</sub>, varying from ~0 pptv to >0.4 pptv. The STRAT measurements were likely obtained in a relatively clean pocket of air that was not recently influenced by convection and therefore show very low CHBr<sub>3</sub> concentrations. Secondly, it is possible that uptake of CHBr<sub>3</sub> on canister surfaces contributed to lower observed bromoform concentrations in the upper troposphere. Though the canisters for STRAT were pre-cleaned with moist air, the treatment of sample canisters for the STRAT mission did not include addition of extra water vapor that became the standard protocol for subsequent missions. The extra water vapor helped minimize adsorptive losses to the canister surfaces.

Due to its longer lifetime, CH<sub>2</sub>Br<sub>2</sub> displays less variability in its atmospheric concentration compared to CHBr<sub>3</sub>. This is clearly seen in lower tropospheric distribution (Fig. 8) as well as vertical profile (Figs. 9 and 10) observed during previous aircraft missions. Annual mean mixing ratios of CH<sub>2</sub>Br<sub>2</sub> are ~1 pptv throughout the troposphere with weak vertical gradients near the surface (Fig. 9). The mean mixing ratio of CH<sub>2</sub>Br<sub>2</sub> is ~0.5 pptv near the tropical tropopause (Fig. 10). Most of the variability in the troposphere is tied to the seasonality in lifetime due to higher rates of reaction with OH in warmer seasons.

The model reproduces well the observed horizontal distribution of CH<sub>2</sub>Br<sub>2</sub> in the lower troposphere (Fig. 8,  $r = 0.78$ ) as well as the vertical gradient in the free troposphere (Fig. 9). Sensitivity simulations show that, unlike CHBr<sub>3</sub>,

CH<sub>2</sub>Br<sub>2</sub> is not sensitive to details in the open ocean vs. coastal proportion in emission distribution. This is consistent with the fact that CH<sub>2</sub>Br<sub>2</sub> has a relatively long lifetime and is more uniformly mixed. Yet its lifetime is short enough to differentiate emissions between tropics, middle latitudes, and high latitudes. An accurate latitudinal distribution in emission is important in reproducing the atmospheric concentration and vertical gradient of CH<sub>2</sub>Br<sub>2</sub> at the corresponding latitudes. While we did not derive an emission distribution specifically for CH<sub>2</sub>Br<sub>2</sub>, our simulated CH<sub>2</sub>Br<sub>2</sub> and its vertical gradient matches well with observations. This is consistent with the fact that both are emitted from the same ocean macroalgae and their atmospheric concentrations are highly correlated (Yokouchi et al., 2005).

Simulated CH<sub>2</sub>Br<sub>2</sub> agrees well with the UT/LS observations below 150 hPa, but is generally too high compared with those between 50–150 hPa, except during Pre-AVE (Fig. 10). While the observed CH<sub>2</sub>Br<sub>2</sub> show significant interannual variation (varying between 0.3–0.6 pptv at 100 hPa from individual missions), the simulated CH<sub>2</sub>Br<sub>2</sub> vary little (<0.1 pptv) from year to year. The model overestimate is likely due to the simplification of using the same zonal-averaged 2-dimensional monthly mean OH fields for each year. However, the fact that simulated CH<sub>2</sub>Br<sub>2</sub> shows a consistent high bias between 50–150 hPa during most of the missions suggests our OH is possibly low compared to mean conditions.

#### 4.2 Impact of emission

In this section, we examine the impact of differences in emission on atmospheric concentrations of CHBr<sub>3</sub> and CH<sub>2</sub>Br<sub>2</sub>.

Figure 11 compares the annual mean CHBr<sub>3</sub> from year 3 of simulations A, B, and C. Simulations B and C reproduce relatively well the observed high concentration band in the tropics, but the band (CHBr<sub>3</sub> > 1 pptv) is too wide compared to observations due to reasons discussed above (Sect. 3). The simulated concentrations at the mid and high latitudes are

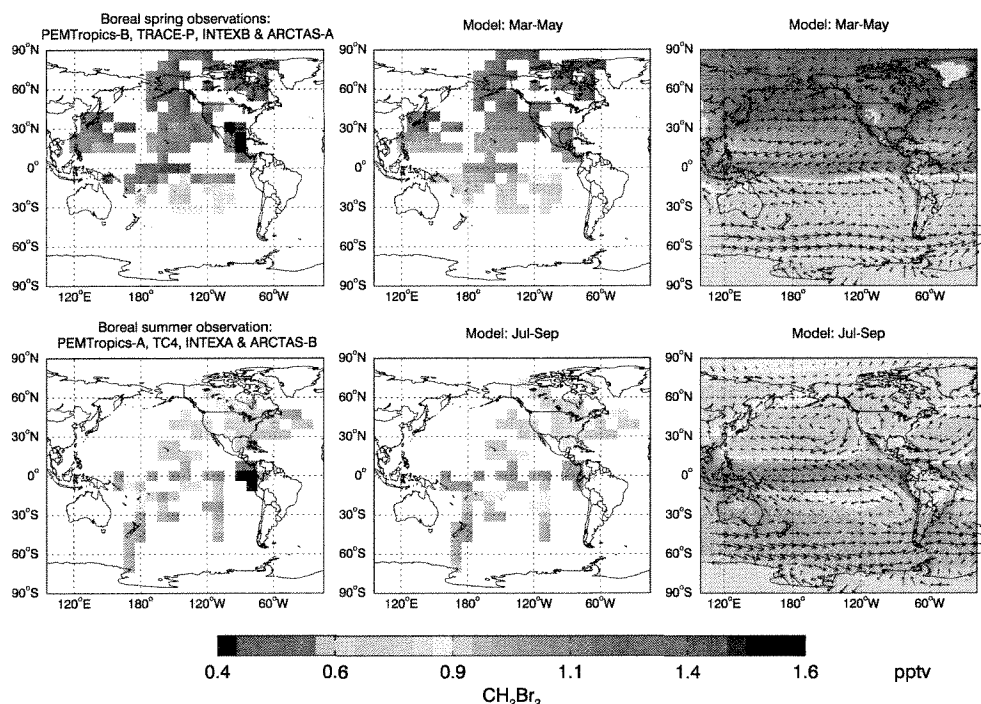


Fig. 8. Same as Fig. 4 but for CH<sub>2</sub>Br<sub>2</sub>.

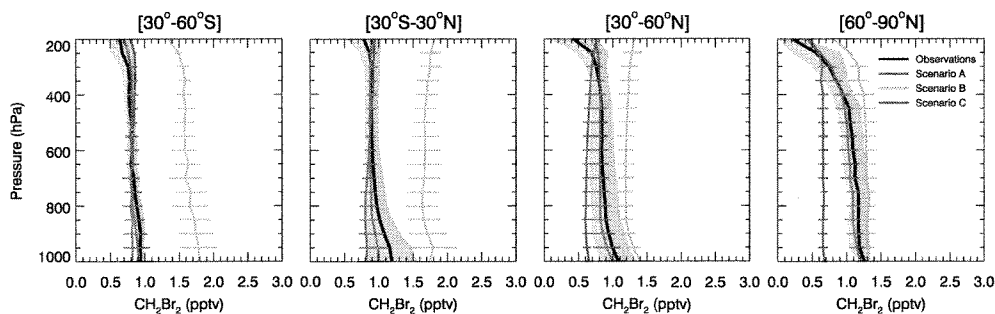


Fig. 9. Comparison between the observed and simulated vertical profiles of CH<sub>2</sub>Br<sub>2</sub> in the troposphere. Observations from all available aircraft missions are averaged for 30–60° S, 30° S–30° N, 30–60° N, and 60–90° N latitude bands at 1-km vertical interval. Black lines show the mean concentrations with gray shadings indicate one standard deviation. The mean CH<sub>2</sub>Br<sub>2</sub> vertical profiles from three simulations are plotted in color with horizontal bars indicating one standard deviation. Model is sampled at the same location as the observations in the corresponding month.

significantly lower than that from simulation A. This inadequacy in the latitudinal gradient of CHBr<sub>3</sub> is also apparent when compared to surface measurements (Fig. 5). Simulations B and C also have difficulty in reproducing the vertical gradient of CHBr<sub>3</sub> for aircraft missions that took place at the middle and high latitudes (Fig. 6). These simulation biases are due to an underestimate in oceanic emission at the corresponding latitudes. Sensitivity simulations show that as a result of its short lifetime, the influence of surface CHBr<sub>3</sub> emissions does not extend far, either horizontally or vertically. To

reproduce the observed vertical profile, it is necessary to have oceanic emission underneath or in adjacent regions. The rate that CHBr<sub>3</sub> concentration falls off with altitude is sensitive to the emission magnitude, and thus is a useful constraint to derive emission strength in the corresponding region. Interestingly, while all three simulations have quite different emissions, they reproduce well the observed vertical profiles of CHBr<sub>3</sub> during PEM-Tropics A and B in the central and southern Pacific (Fig. 6). This is consistent with the results in Warwick et al. (2006), who found both Scenarios B and C

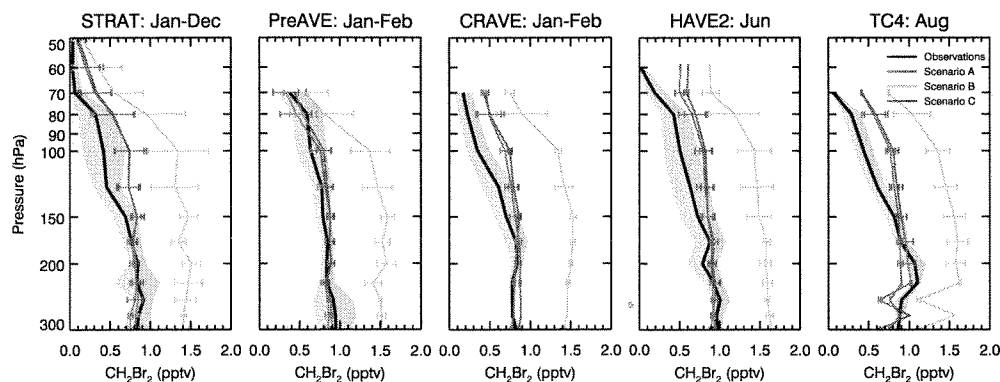


Fig. 10. Same as Fig. 6 but for CH<sub>2</sub>Br<sub>2</sub> in the UT/LS region.

yield a good match with observations. While the simulated CHBr<sub>3</sub> from simulation C agrees well with the tropical open ocean observations obtained during PEM-Tropics, it is too high compared with the troposphere/lower stratosphere measurements obtained during TC4, Pre-AVE, and HAVE2 along the tropical west coast of South America (Figs. 6 and 7). This implies that the 280 Gg Br yr<sup>-1</sup> tropical coastal emissions used in Scenario C is likely too high. This agrees with the results from Kerkweg et al. (2008) who found that with emission Scenario 5 from Warwick et al. (2006) (Scenario C in the study), the simulated CHBr<sub>3</sub> is too high compared to observations in the UT/LS.

The simulated CH<sub>2</sub>Br<sub>2</sub> concentration is sensitive to the magnitude of global emission as well as latitudinal distribution. Simulation B produces much higher CH<sub>2</sub>Br<sub>2</sub> concentrations compared with the observations and the other two simulations in most of the troposphere and LS except in the northern high latitudes (Figs. 9 and 10). The global emission of 104 Gg Br yr<sup>-1</sup> used in simulation B was deduced in Warwick et al. (2006) by matching the background atmospheric concentrations. Kerkweg et al. (2008) also found that their simulated CH<sub>2</sub>Br<sub>2</sub> with the global emission estimate suggested by Warwick et al. (2006) is too high compared against the vertical profiles obtained during PEM-Tropics A and B. The difference is most likely due to differences in the OH fields in individual models. OH in the atmosphere is controlled by various chemical and moist physical processes and an accurate representation of OH in global chemistry remains an active yet challenging research task. The difference between simulation A and C (Fig. 9) illustrates the sensitivity of atmospheric CH<sub>2</sub>Br<sub>2</sub> mixing ratios to emission at the corresponding latitudes. While CH<sub>2</sub>Br<sub>2</sub> displays a much weaker vertical gradient compared to CHBr<sub>3</sub>, its vertical gradient is a useful indicator of surface emissions, similar to CHBr<sub>3</sub>. With little emissions in the mid and high latitudes (simulation C), it is difficult to reproduce the observed concentrations as well as the vertical gradients.

The above suggests that top-down emission estimate of short-lived bromocarbons are subject to great uncertainties introduced by the abundance of available measurements, both spatially and temporally, and model OH fields. For CHBr<sub>3</sub>, which has a relatively short lifetime and loss occurs dominantly via photolysis, the derived estimate is dependent on the observations used. The uncertainty can be significantly reduced when there are more measurements available, particularly over the strong emission regions, e.g. along the coasts and near the equatorial tropics. Dibromomethane has a relatively long lifetime and is well-mixed in the troposphere, with loss occur predominantly via reaction with OH. Thus, uncertainty in the top-down emission estimate of CH<sub>2</sub>Br<sub>2</sub> is mostly associated with the calculated rate of loss against OH. Differences between this study and that from Warwick et al. (2006) suggest that the uncertainty can be as high as 100%, most likely due to differences in OH. Top-down emission estimates for CHBrCl<sub>2</sub>, CHBr<sub>2</sub>Cl and CH<sub>2</sub>BrCl are subject to similar uncertainties as their loss occurs dominantly through reaction with OH. Results from this study also indicates that while the observed vertical gradient is a useful constraint in deriving surface emissions as shown by many previous studies, it is helpful to combine vertical profiles with horizontal distributions to achieve an accurate emission estimate globally and a better understanding of possible model bias.

## 5 The contribution of short-lived bromocarbons to stratospheric bromine

The simulated CHBr<sub>3</sub> and CH<sub>2</sub>Br<sub>2</sub> concentrations in the troposphere reach steady state in about or less than one year. In contrast, their impact on total bromine levels in the stratosphere, particularly Br<sub>y</sub>, approaches steady state much more slowly, a result of slow transport in the stratosphere. Figure 12 shows the temporal increment of total bromine (organic and inorganic) produced from VSL bromocarbons

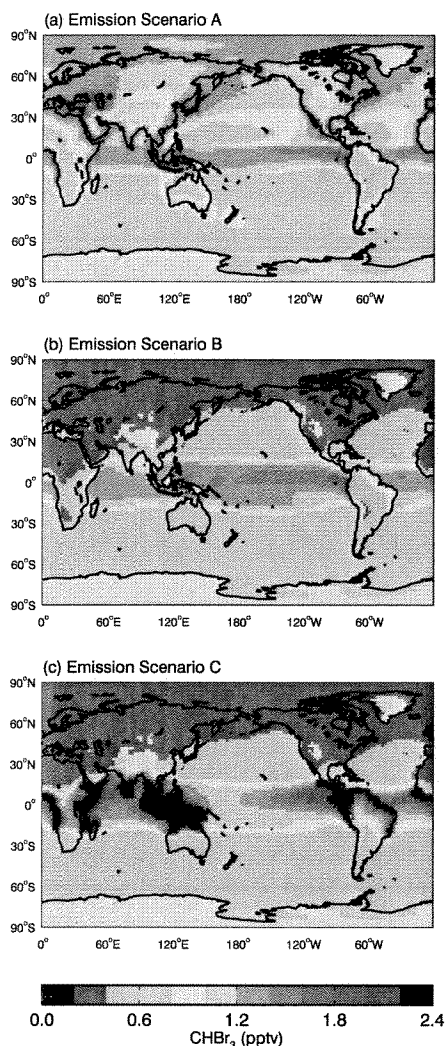


**Fig. 11.** The annual mean horizontal distribution of CHBr<sub>3</sub> in the lower troposphere (1000–800 hPa) from simulations conducted with emission (a) Scenario A, (b) Scenario B, and (c) Scenario C.

(Br<sup>VLSL</sup>) at different locations in the stratosphere. Br<sup>VLSL</sup> near the tropical tropopause (0° N, 100 hPa) reaches steady state concentration at the end of year 2 while that near the mid/high latitude tropopause and in the tropical mid/upper stratosphere gradually increases. The entire stratosphere approaches steady state at year 12. The zonal averaged Br<sup>VLSL</sup> from year 3 of the simulation shows that the troposphere-to-stratosphere transport of Br<sup>VLSL</sup> occurs via vertical advection into the tropical stratosphere and quasi-horizontal isentropic transport into the mid-latitude lower stratosphere (Fig. 13c), similar to results from Nielsen and Douglass (2001). The middle and high latitude lower stratosphere is controlled by the relatively rapid quasi-horizontal cross-tropopause isentropic transport from the tropical troposphere and the slower

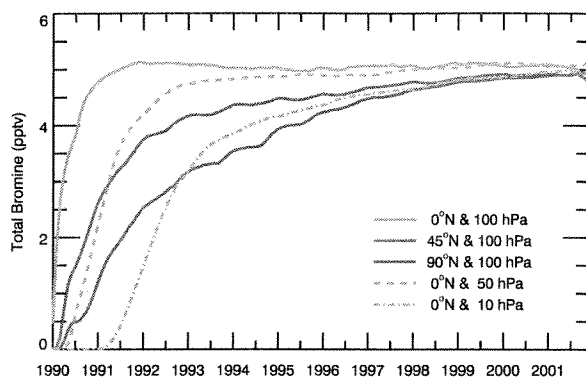


**Fig. 12.** Simulated total bromine at 100 hPa (gray solid line), 50 hPa (gray dashed line), and 10 hPa (gray dash-dotted line) at the equator, as well as those at 45° N (red) and 90° N (blue) at 100 hPa between January 1990 and December 2001. We apply a 13-month running mean filter to each monthly-mean time series to remove seasonal variations.

descending motion associated with the mean meridional circulation (Nielsen and Douglass, 2001). As a result, Br<sup>VLSL</sup> in the middle/high latitude lower stratosphere increases rapidly at the beginning of the simulation and approaches steady state more slowly than that at the equatorial middle and high stratosphere (Fig. 12).

Figures 13d–f and 14 present the steady-state contribution of CHBr<sub>3</sub> and CH<sub>2</sub>Br<sub>2</sub> to bromine in the atmosphere. At steady state, inclusion of CHBr<sub>3</sub> and CH<sub>2</sub>Br<sub>2</sub> adds a uniform ~5 pptv to total bromine in the entire stratosphere, set by Br<sup>VLSL</sup> concentration at the entry point – the tropical tropopause layer. Previous modeling studies with 3–4 years of simulation length suggested that contribution of very short-lived bromocarbons to inorganic bromine in the stratosphere peaks at a certain altitude in the stratosphere (e.g. Nielsen and Douglass, 2001; Warwick et al., 2006). However, our results demonstrate that this is merely a snapshot contribution amid the spin-up process. As we can clearly see in Fig. 13b, at year 3, Br<sub>y</sub><sup>VLSL</sup> peaks in the tropical lower stratosphere. As the simulation continues, the maximum Br<sub>y</sub><sup>VLSL</sup> area extends further both horizontally and vertically until reaching steady state concentration throughout the entire stratosphere.

Troposphere-to-stratosphere transport of source gases and their degradation products are equally important. Inorganic bromine accounts for half of Br<sup>VLSL</sup> near the tropopause and its contribution increases rapidly with altitude as source gases quickly photo-dissociate to produce Br<sub>y</sub>. Above 50 hPa, almost all is in the form of Br<sub>y</sub>. The contribution of CH<sub>2</sub>Br<sub>2</sub> to reactive bromine in the stratosphere is of equal or greater importance as that of CHBr<sub>3</sub>. While CHBr<sub>3</sub> contributes mostly via product gas injection, source gas injection is a more important pathway for CH<sub>2</sub>Br<sub>2</sub>. This additional Br<sub>y</sub> produced from the VLSL can have a significant impact

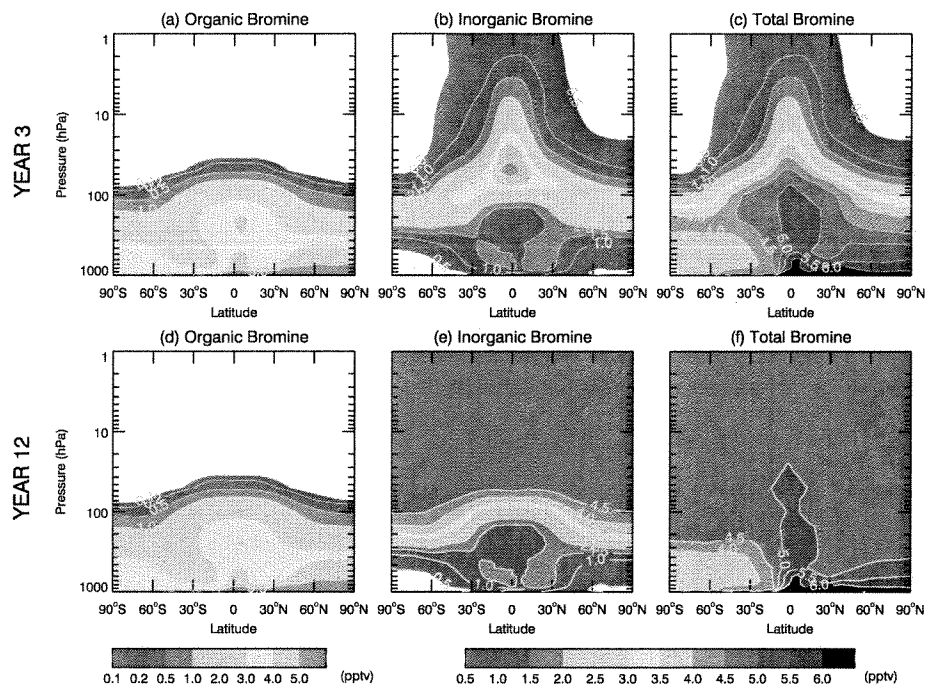


**Fig. 13.** The latitude-pressure cross section of the contribution of  $\text{CHBr}_3$  and  $\text{CH}_2\text{Br}_2$  to organic bromine (left column), inorganic bromine (middle column) and total bromine (right column) from year 3 and year 12 of the simulation.

on stratospheric ozone depletion. The associated BrO cause more ozone depletion due to enhanced catalytic loss by the BrO+ClO cycle (Salawitch et al., 2005). Secondly, an addition of  $\sim 5$  pptv of Br<sub>y</sub> causes the photochemical loss of ozone by BrO+HO<sub>2</sub> cycle to be of considerable importance below  $\sim 14$  km (Salawitch et al., 2005).

About 30% of the Br<sub>y</sub> produced from  $\text{CHBr}_3$  and  $\text{CH}_2\text{Br}_2$  in the troposphere is removed by wet scavenging, and more than 85% of the wet removal is due to large-scale precipitation below 500 hPa. The mixing ratio of Br<sub>y</sub><sup>VLSL</sup> is relatively constant from the tropical middle troposphere to the stratopause, implying small wet scavenging during troposphere-to-stratosphere transport. We conducted a 12-year sensitivity simulation without wet scavenging in convective updrafts and found that convective scavenging only accounts for  $\sim 0.2$  pptv (4%) difference in Br<sub>y</sub><sup>VLSL</sup> in the stratosphere, contrary to the conventional wisdom. This result agrees with the sensitivity study of Dvortsov et al. (1999), who found that estimates of Br<sub>y</sub> in the lowermost stratosphere are not very sensitive to convection. Mixing ratios of a chemical species entering the stratosphere is determined by its photochemistry and dehydration processes during troposphere-to-stratosphere transport through the TTL (Sinnhuber and Folkins, 2006; Fueglistaler et al., 2009). Based on the tropical vertical profiles of Br<sub>y</sub><sup>VLSL</sup> (Fig. 14), we can deduce that about 3 pptv of the stratospheric Br<sub>y</sub><sup>VLSL</sup> is formed either in the stratosphere or in

the TTL above the level of neutral buoyancy (LNB) (potential temperature  $\sim 355$  K and  $\sim 125$  hPa) where they can enter the stratosphere via radiative ascent (Fueglistaler et al., 2009), and are therefore not subject to convective scavenging. The remaining  $\sim 2$  pptv are formed below the TTL. The results from our detailed wet deposition scheme, which includes rainout/washout, convective scavenging and evaporation, suggests that dehydration during troposphere-to-stratosphere transport occurs slowly so that most of the Br<sub>y</sub><sup>VLSL</sup> that is lofted in convective updrafts is released back to the atmosphere during evaporation, subsequently escaping to the stratosphere.

Our estimate of  $\sim 5$  pptv contribution of  $\text{CHBr}_3$  and  $\text{CH}_2\text{Br}_2$  to stratospheric bromine agrees well with previous ground and balloon-borne measurements ( $\sim 5$  pptv) (Sinnhuber et al., 2002; Dorf et al., 2008) as well as satellite observations (3–8 pptv) (Sinnhuber et al., 2005; Livesey et al., 2006; Sioris et al., 2006). This estimate is similar to that from Warwick et al. (2006) (6–7 pptv for all five VSL bromocarbons), but in general higher than many previous modeling estimates that between 0.7–1.8 pptv for  $\text{CHBr}_3$  alone (Dvortsov et al., 1999; Nielsen and Douglass, 2001; Hossaini et al., 2010) and 2.4–2.8 pptv for  $\text{CHBr}_3$  and  $\text{CH}_2\text{Br}_2$  combined (Gettelman et al., 2009; Hossaini et al., 2010). The difference is mostly due to differences in the rate of wet scavenging, which is  $\sim 50\%$  lower in the GEOS CCM (wet deposition lifetime  $\sim 15$  days) than most models (wet deposition lifetime of 10 days). While

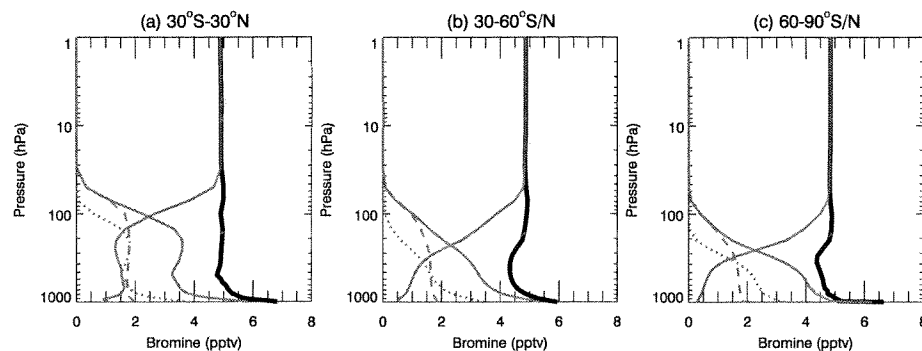


**Fig. 14.** The model calculated contribution of organic bromine (red solid lines), inorganic bromine (blue lines), and total bromine (black lines) from short-lived bromocarbons, averaged between (a) 30° S–30° N, (b) 30–60° S/N, and (c) 60–90° S/N. The relative contribution of bromine from CHBr<sub>3</sub> (CHBr<sub>3</sub>×3, red dotted lines) and CH<sub>2</sub>Br<sub>2</sub> (CH<sub>2</sub>Br<sub>2</sub>×2, red dashed lines) to organic bromine is also included.

Warwick et al. (2006) uses the same wet deposition rate as the other models, the impact of higher emissions cancels off with the impact of faster scavenging and yields a comparable contribution as this study. Similarly, our estimated contribution due to injection of product gases which are subject to wet scavenging (~50% for CHBr<sub>3</sub> and CH<sub>2</sub>Br<sub>2</sub> combined) is also significantly higher than the ~50% for CHBr<sub>3</sub> (Dvortsov et al., 1999; Nielsen and Douglass, 2001; Hossaini et al., 2010) and ~90% for CH<sub>2</sub>Br<sub>2</sub> (Hossaini et al., 2010) from previous modeling analysis.

## 6 Conclusions

We performed a modeling study using the GEOS CCM to quantify the contribution of CHBr<sub>3</sub> and CH<sub>2</sub>Br<sub>2</sub> to reactive bromine in the stratosphere. We conducted a 12-year bromocarbon simulation that includes a detailed representation of oceanic emissions of CHBr<sub>3</sub> and CH<sub>2</sub>Br<sub>2</sub>, their chemical losses through photolysis and reaction with OH, surface dry deposition of inorganic bromine (their degradation product), and wet scavenging of inorganic bromine in large-scale precipitation and convective updrafts.

We used observed concentrations and vertical profiles of CHBr<sub>3</sub> and CH<sub>2</sub>Br<sub>2</sub> from previous NASA aircraft campaigns, including PEM-tropics, TRACE-P, INTEX, ARCTAS, TC4, STRAT, Pre-AVE and AVE, to derive a top-down emission estimate of CHBr<sub>3</sub> and CH<sub>2</sub>Br<sub>2</sub> from oceanic sources. To produce the observed background mixing ratios, we estimated that the global emissions of CHBr<sub>3</sub> and CH<sub>2</sub>Br<sub>2</sub> are 425 Gg Br yr<sup>-1</sup> and 57 Gg Br yr<sup>-1</sup>, respectively, with 60% from open ocean and 40% from coastlines. Our emission estimates agree well with previous modeling estimates and are within the uncertainty range of bottom-up emission estimates. The 425 Gg Br yr<sup>-1</sup> for CHBr<sub>3</sub> is likely a lower limit as the model does not reproduce the very high mixing ratios observed in the marine boundary layer. Our

sensitivity simulations indicate that top-down emission estimate for CH<sub>2</sub>Br<sub>2</sub> is sensitive to model representation of atmospheric OH concentration as reaction with OH is the dominant process for degradation of CH<sub>2</sub>Br<sub>2</sub>.

When initialized with zero atmospheric concentrations, the distribution of bromocarbon source gases and the resulted inorganic bromine to the stratosphere approach steady state in ~12 years. At steady state, including CHBr<sub>3</sub> and CH<sub>2</sub>Br<sub>2</sub> adds a ubiquitous ~5 pptv to total bromine (organic and inorganic) in the stratosphere, with transport of source gases and transport of their degradation product being equally important. Inorganic bromine accounts for a half (~2.5 pptv) of total bromine from the VSL bromocarbons near the tropopause. Its contribution increases rapidly with altitude and reaches a constant ~5 pptv at 50 hPa and above, which can have a significant impact on stratospheric ozone depletion.

Bromoform has been suggested to play the most important role among short-lived oceanic bromocarbons in contributing reactive bromine to the stratosphere. Our results indicate that CH<sub>2</sub>Br<sub>2</sub> is of equal or greater importance. While CHBr<sub>3</sub> contributes mostly via product gas injection, source gas injection is a more important pathway for CH<sub>2</sub>Br<sub>2</sub>.

More than 85% of the wet scavenging of Br<sub>y</sub><sup>VSL</sup> occurs below 500 hPa due to large-scale precipitation. Great emphasis has been placed on the impact of convective transport on the troposphere-to-stratosphere transport of the VSL bromocarbons and wet scavenging of the resulted inorganic bromine. However, our sensitivity study shows that convective scavenging only accounts for ~0.2 pptv (4%) difference in inorganic bromine delivered to the stratosphere due to dominant source gas injection above neutral buoyancy level in the tropical tropopause layer and slow dehydration during lofting in deep convection.

**Acknowledgements.** This research was supported by an appointment to the NASA Postdoctoral Program at the Goddard Space Flight Center, administered by Oak Ridge Associated Universities through a contract with NASA. We thank Stephan Fueglistaler for helpful discussions on transport in the tropical tropopause layer. We also acknowledge the useful comments from two anonymous reviewers.

Edited by: L. Carpenter

## References

- Aschmann, J., Sinnhuber, B.-M., Atlas, E. L., and Schauffler, S. M.: Modeling the transport of very short-lived substances into the tropical upper troposphere and lower stratosphere, *Atmos. Chem. Phys.*, 9, 9237–9247, 2009, <http://www.atmos-chem-phys.net/9/9237/2009/>.
- Atlas, E., Pollock, W., Greenberg, J., Heidt, L., and Thompson, A. M.: Alkyl Nitrates, Nonmethane Hydrocarbons, and Halocarbon Gases Over the Equatorial Pacific Ocean During Saga 3, *J. Geophys. Res.*, 98(D9), 16933–16947, 1993.
- Atlas, E. L. and Ridley, B. A.: The Mauna Loa Observatory Photochemistry Experiment: Introduction, *J. Geophys. Res.*, 101, 14531–14541, 1996.
- Balkanski, Y. J., Jacob, D. J., Gardner, G. M., Graustein, W. C., and Turekian, K. K.: Transport and residence times of tropospheric aerosols inferred from a global three-dimensional simulation of <sup>210</sup>Pb, *J. Geophys. Res.*, 98, 20573–20586, 1993.
- Bey, I., Jacob, D. J., Yantosca, R. M., Logan, J. A., Field, B. D., Fiore, A. M., Li, Q., Liu, H. Y., Mickley, L. J., and Schultz, M. G.: Global modeling of tropospheric chemistry with assimilated meteorology: Model description and evaluation, *J. Geophys. Res.*, 106, 23073–23096, 2001.
- Blake, N. J., Blake, D. R., Simpson, I. J., et al.: NMHCs and halocarbons in Asian continental outflow during TRACE-P: Comparison to PEM-WestB, *J. Geophys. Res.*, 108(D20), 8806, doi:10.1029/2002JD003367, 2003.
- Butler, J. H., King, D. B., Montzka, S. A., Lobert, J. M., Yvon-Lewis, S. A., and Warwick, N. J.: Oceanic fluxes of CHBr<sub>3</sub>, CH<sub>2</sub>Br<sub>2</sub>, and CH<sub>3</sub>I into the marine boundary layer, *Global Biogeochem. Cy.*, 21, GB1023, doi:10.1029/2006GB002732, 2007.
- Carpenter, L. J. and Liss, P. S.: On temperate sources of Bromoform and other reactive organic bromine gases, *J. Geophys. Res.*, 105(D16), 20539–20547, 2000.
- Carpenter, L. J., Sturges, W. T., Liss, P. S., Penkett, S. A., Alicke, B., Hebestreit, K., and Platt U.: Short-lived alkyl iodides and bromides at Mace Head, Ireland: Links to biogenic sources and halogen oxide production, *J. Geophys. Res.*, 104, 1679–1690, 1999.
- Carpenter, L. J., Malin, G., Kuepper, F., and Liss, P. S.: Novel biogenic iodine-containing trihalomethanes and other short-lived halocarbons in the coastal East Atlantic, *Global Biogeochem. Cy.*, 14, 1191–1204, 2000.
- Carpenter, L. J., Wevill, D. J., Hopkins, J. R., Dunk, R. M., Jones, C. E., Hornsby, K. E., and McQuaid, J. B.: Bromoform in tropical Atlantic air from 25° N to 25° S, *Geophys. Res. Lett.*, 34, L11810, doi:10.1029/2007GL029893, 2007.
- Carpenter, L. J., Jones, C. E., Dunk, R. M., Hornsby, K. E., and Woeltjen, J.: Air-sea fluxes of biogenic bromine from the tropical and North Atlantic Ocean, *Atmos. Chem. Phys.*, 9, 1805–1816, 2009, <http://www.atmos-chem-phys.net/9/1805/2009/>.
- Chin, M., Rood, R. B., Lin, S.-J., Muller, J. F., and Thomsson, A. M.: Atmospheric sulfur cycle in the global model GOCART: Model description and global properties, *J. Geophys. Res.*, 105, 24671–24687, 2000a.
- Chin, M., Savoie, D. L., Huebert, B. J., Bandy, A. R., Thornton, D. C., Bates, T. S., Quinn, P. K., Saltzman, E. S., and De Bruyn, W. J.: Atmospheric sulfur cycle in the global model GOCART: Comparison with field observations and regional budgets, *J. Geophys. Res.*, 105, 24689–24712, 2000b.
- Chin, M., Diehl, T., Ginoux, P., and Malm, W.: Intercontinental transport of pollution and dust aerosols: implications for regional air quality, *Atmos. Chem. Phys.*, 7, 5501–5517, 2007, <http://www.atmos-chem-phys.net/7/5501/2007/>.
- Class, Th., Kohnle, R., and Ballschmiter, K.: Chemistry of organic traces in air, VII, Bromo- and bromochloromethanes in air over the Atlantic Ocean, *Chemosphere*, 15(4), 429–436, 1986.
- Dorf, M., Butz, A., Camy-Peyret, C., Chipperfield, M. P., Kritten, L., and Pfeilsticker, K.: Bromine in the tropical troposphere and stratosphere as derived from balloon-borne BrO observations, *Atmos. Chem. Phys.*, 8, 7265–7271, 2008, <http://www.atmos-chem-phys.net/8/7265/2008/>.
- Douglass, A. R. and Kawa, S. R.: Contrast between 1992 and 1997 high-latitude spring Halogen Occultation Experiment observations of lower stratospheric HCl, *J. Geophys. Res.*, 104(D15), 18739–18754, doi:10.1029/1999JD900281, 1999.
- Douglass, A. R., Stolarski, R. S., Schoeberl, M. R., Jackman, C. H., Gupta, M. L., Newman, P. A., Nielsen, J. E., and Fleming, E. L.: Relationship of loss, mean age of air and the distribution of CFCs to stratospheric circulation and implications for atmospheric lifetimes, *J. Geophys. Res.*, 113, D14309, doi:10.1029/2007JD009575, 2008.
- Dvortsov, V. L., Geller, M. A., Solomon, S., Schauffler, S. M., Atlas, E. L., and Blake, D. R.: Rethinking reactive halogen budgets in the midlatitudes lower stratosphere, *Geophys. Res. Lett.*, 26, 1699–1702, 1999.
- Eyring, V., Butchart, N., Waugh, D. W., et al.: Assessment of temperature, trace species, and ozone in chemistry-climate model simulations of the recent past, *J. Geophys. Res.*, 111, D22308, doi:10.1029/2006JD007327, 2006.
- Fueglistaler, S., Bonazzola, M., Haynes, P. H., and Peter, T.: Stratospheric water vapor predicted from the Lagrangian temperature history of air entering the stratosphere in the tropics, *J. Geophys. Res.*, 110, D08107, doi:10.1029/2004JD005516, 2005.
- Fueglistaler, S., Dessler, A. E., Dunkerton, T. J., Folkins, I., Fu, Q., and Mote, P. W.: Tropical tropopause layer, *Rev. Geophys.*, 47(1), RG1004, doi:10.1029/2008RG000267, 2009.
- García, R. R., and Solomon, S.: A new numerical model of the middle atmosphere: 2. Ozone and related species, *J. Geophys. Res.*, 99, 12,937–12,951, 1994.
- Gettelman, A., Lauritzen, P. H., Park, M., and Kay, J. E.: Processes regulating short-lived species in the tropical tropopause layer, *J. Geophys. Res.*, 114, D13303, doi:10.1029/2009JD011785, 2009.
- Ginoux, P., Chin, M., Tegen, I., Prospero, J., Holben, B., Dubovik, O., and Lin, S.-J.: Sources and distributions of dust aerosols simulated with the GOCART model, *J. Geophys. Res.*, 106, 20225–20273, 2001.



- Giorgi, F. and Chameides, W. L.: Rainout lifetimes of highly soluble aerosols and gases as inferred from simulations with a general circulation model, *J. Geophys. Res.*, 91, 14367–14376, 1986.
- Goodwin, K. D., Lidstrom, M. E., and Oremland, R. S.: Marine bacterial degradation of brominated methanes, *Environ. Sci. Technol.*, 31, 3188–3192, 1997.
- Hoell, J. M., Davis, D. D., Jacob, D. J., Rodgers, M. O., Newell, R. E., Fuelberg, H. E., McNeal, R. J., Raper, J. L., and Bendura, R. J.: Pacific Exploratory Mission in the tropical Pacific: PEM-Tropics A, August–September 1996, *J. Geophys. Res.*, 104(D5), 5567–5583, 1999.
- Holton, J. R. and Gettelman, A.: Horizontal transport and the dehydration of the stratosphere, *Geophys. Res. Lett.*, 28, 2799–2802, 2001.
- Hossaini, R., Chipperfield, M. P., Monge-Sanz, B. M., Richards, N. A. D., Atlas, E., and Blake, D. R.: Bromoform and dibromomethane in the tropics: a 3-D model study of chemistry and transport, *Atmos. Chem. Phys.*, 10, 719–735, 2010, <http://www.atmos-chem-phys.net/10/719/2010/>.
- Jacob, D. J., Crawford, J. H., Kleb, M. M., Connors, V. S., Bendura, R. J., Raper, J. L., Sachse, G. W., Gille, J. C., Emmons, L., and Heald, C. L.: Transport and Chemical Evolution over the Pacific (TRACE-P) aircraft mission: Design, execution, and first results, *J. Geophys. Res.*, 108(D20), 9000, doi:10.1029/2002JD003276, 2003.
- Jacob, D. J., Crawford, J. H., Maring, H., Clarke, A. D., Dibb, J. E., Ferrare, R. A., Hostetler, C. A., Russell, P. B., Singh, H. B., Thompson, A. M., Shaw, G. E., McCauley, E., Pederson, J. R., and Fisher, J. A.: The ARCTAS aircraft mission: design and execution, *Atmos. Chem. Phys. Discuss.*, 9, 17073–17123, 2009, <http://www.atmos-chem-phys-discuss.net/9/17073/2009/>.
- Kerkweg, A., Jöckel, P., Warwick, N., Gebhardt, S., Brenninkmeijer, C. A. M., and Lelieveld, J.: Consistent simulation of bromine chemistry from the marine boundary layer to the stratosphere – Part 2: Bromocarbons, *Atmos. Chem. Phys.*, 8, 5919–5939, 2008, <http://www.atmos-chem-phys.net/8/5919/2008/>.
- Klick, S.: The release of volatile halocarbons to seawater by untreated and heavy metal exposed samples of the brown seaweed, *Fucus vesiculosus*, *Mar. Chem.*, 42, 211–221, 1993.
- Kroon, M., Petropavlovskikh, I., Shetter, R., Hall, S., Ullmann, K., Veefkind, J. P., McPeters, R. D., Browell, E. V., and Levelt, P. F.: OMI total ozone column validation with Aura-AVE CAFS observations, *J. Geophys. Res.*, 113, D15S13, doi:10.1029/2007JD008795, 2008.
- Kurylo, M. J. and Rodriguez, J. M.: Short-lived ozone related compounds, in *Scientific Assessment of Ozone Depletion: 1998*, Global Ozone Res. and Monit. Proj., Rep. 44, chap. 2, World Meteorol. Organ., Geneva, Switzerland, 1999.
- Liang, Q., Jaeglé, L., Hudman, R. C., et al.: Summertime influence of Asian pollution in the free troposphere over North America, *J. Geophys. Res.*, 112, D12S11, doi:10.1029/2006JD007919, 2007.
- Liang, Q., Stolarski, R. S., Douglass, A. R., Newman, P. A., and Nielsen, J. E.: Evaluation of emissions and transport of CFCs using surface observations and their seasonal cycles and the GEOS CCM simulation with emissions-based forcing, *J. Geophys. Res.*, 113, D14302, doi:10.1029/2007JD009617, 2008.
- Lin, S.-J.: A “vertically Lagrangian” finite-volume dynamical core for global models, *Mon. Weather Rev.*, 132(10), 2293–2307, 2004.
- Livesey, N. J., Kovalenko, L. J., Salawitch, R. J., MacKenzie, I. A., Chipperfield, M. P., Read, W. G., Jarnot, R. F., and Waters, J. W.: EOS Microwave Limb Sounder observations of upper stratospheric BrO: Implications for bromine, *Geophys. Res. Lett.*, 33, L20817, doi:10.1029/2006GL026930, 2006.
- McElroy, M., Salawitch, R. J., Wolfsy, S., and Logan, J.: Reductions of Antarctic ozone due to synergistic interactions of chlorine and bromine, *Nature*, 321, 759–762, 1986.
- Moorthi, S. and Suarez, M. J.: Relaxed Arakawa-Schubert: A parameterization of moist convection for general circulation models, *Mon. Weather Rev.*, 120, 978–1002, 1992.
- Nielsen, J. E. and Douglass, A. R.: A simulation of bromoform’s contribution to stratospheric bromine, *J. Geophys. Res.*, 106, 8089–8100, 2001.
- Ott, L. E., Pawson, S., and Bacmeister, J.: An analysis of the impact of convective parameter sensitivity on simulated global atmospheric CO distributions, in preparation, 2010.
- Pawson, S., Stolarski, R. S., Douglass, A. R., Newman, P. A., Nielsen, J. E., Frith, S. M., and Gupta, M. L.: Goddard Earth Observing System Chemistry–Climate Model Simulations of Stratospheric Ozone–Temperature Coupling Between 1950 and 2005, *J. Geophys. Res.*, 113, D12103, doi:10.1029/2007JD009511, 2008.
- Quack, B. and Wallace, D. W. R.: Air-sea flux of bromoform: Controls, rates and implications, *Global Biogeochem. Cy.*, 17(1), 1023, doi:10.1029/2002GB001890, 2003.
- Quack, B., Atlas, E., Petrick, B., Stroud, V., Schauffler, S., and Wallace, D. W.: Oceanic bromoform sources for the tropical atmosphere, *Geophys. Res. Lett.*, 31, L23S05, doi:10.1029/2004GL020597, 2004.
- Quack, B., Atlas, E., Petrick, G., and Wallace, D. W. R.: Bromoform and dibromomethane above the Mauritanian upwelling: Atmospheric distributions and oceanic emissions, *J. Geophys. Res.*, 112(D9), D09312, doi:10.1029/2006JD007614, 2007.
- Raper, J., Kleb, M. M., Jacob, D. J., Davis, D. D., Newell, R. E., Fuelberg, H. E., Bendura, R. J., Hoell, J. M., and McNeal, R. J.: Pacific Exploratory Mission in the Tropical Pacific: PEM-Tropics B, March–April 1999, *J. Geophys. Res.*, 106(D23), 32401–32425, 2001.
- Reinecker, M. M., Suarez, M. J., Todling, R., et al.: The GEOS-5 Data Assimilation System–Documentation of Versions 5.0.1, 5.1.0, and 5.2.0, Tech. Rep. 104606 V27, NASA, Greenbelt, MD, 2008.
- Salawitch, R. J., Weisenstein, D. K., Kovalenko, L. J., Sioris, C. E., Wennberg, P. O., Chance, K., Ko, M. K. W., and McLinden, C. A.: Sensitivity of ozone to bromine in the lower stratosphere, *Geophys. Res. Lett.*, 32, L05811, doi:10.1029/2004GL021504, 2005.
- Schauffler, S. M., Atlas, E. L., Blake, D. R., Flocke, F., Lueb, R. A., Lee-Taylor, J. M., Stroud, V., and Travnicek, W.: Distributions of brominated organic compounds in the troposphere and lower stratosphere, *J. Geophys. Res.*, 104(D17), 21513–21535, 1999.
- Sherwood, S. C. and Dessler, A. E.: On the control of stratospheric humidity, *Geophys. Res. Lett.*, 27, 2513–2516, 2000.
- Singh, H. B., Brune, W. H., Crawford, J. H., Jacob, D. J., and Russell, P. B.: Overview of the summer 2004 Intercontinental Chemical Transport Experiment–North America (INTEX-A), *J. Geo-*

- phys. Res., 111, D24S01, doi:10.1029/2006JD007905, 2006.
- Singh, H. B., Brune, W. H., Crawford, J. H., Flocke, F., and Jacob, D. J.: Chemistry and transport of pollution over the Gulf of Mexico and the Pacific: spring 2006 INTEX-B campaign overview and first results, *Atmos. Chem. Phys.*, 9, 2301–2318, 2009, <http://www.atmos-chem-phys.net/9/2301/2009/>.
- Sinnhuber, B.-M., Arlander, D. W., Bovensmann, H., et al.: Comparison of measurements and model calculations of stratospheric bromine monoxide, *J. Geophys. Res.*, 107(D19), 4398, doi:10.1029/2001JD000940, 2002.
- Sinnhuber, B.-M., Rozanov, A., Sheode, N., Afe, O. T., Richter, A., Sinnhuber, M., Wittrock, F., Burrows, J. P., Stiller, G. P., von Clarmann, T., and Linden, A.: Global observations of stratospheric bromine monoxide from SCIAMACHY, *Geophys. Res. Lett.*, 32, L20810, doi:10.1029/2005GL023839, 2005.
- Sinnhuber, B.-M. and Folkins, I.: Estimating the contribution of bromoform to stratospheric bromine and its relation to dehydration in the tropical tropopause layer, *Atmos. Chem. Phys.*, 6, 4755–4761, 2006, <http://www.atmos-chem-phys.net/6/4755/2006/>.
- Sioris, C. E., Kovalenko, L. J., McLinden, et al.: Latitudinal and vertical distribution of bromine monoxide in the lower stratosphere from Scanning Imaging Absorption Spectrometer for Atmospheric Chartography limb scattering measurements, *J. Geophys. Res.*, 111, D14301, doi:10.1029/2005JD006479, 2006.
- Solomon, S., Wuebbles, D., Isaksen, I., Kiehl, J., Lal, M., Simon, P., and Sze, N. D.: Ozone depletion potentials, global warming potentials and future chlorine/bromine loading, in *Scientific Assessment of Ozone Depletion: 1994*, Global Ozone Res. and Monit. Proj. Rep. 37, World Meteorol. Organ., Geneva, Switzerland, 13.1–13.36, 1995.
- Sturges, W. T., Cota, G. F., and Buckley, P. T.: Bromoform emission from Arctic ice algae, *Nature*, 358, 6388, 660–662, 1992.
- Sturges, W. T., Cota, G. F., and Buckley, P. T.: Vertical profiles of bromoform in snow, sea ice, and seawater in the Canadian Arctic, *J. Geophys. Res.*, 102(C11), 25073–25083, 1997.
- Sturges, W. T., Oram, D. E., Carpenter, L. J., Penkett, S. A., and Engel, A.: Bromoform as a source of stratospheric bromine, *Geophys. Res. Lett.*, 27(14), 2081–2084, 2000.
- Toon, O. B., Starr, D. O., Jensen, E. J., et al.: Planning, Implementation and First Results of the Tropical Composition, Cloud and Climate Coupling Experiment (TC4), *J. Geophys. Res.*, submitted, 2010.
- Turquety, S., Logan, J. A., Jacob, D. J., et al.: Inventory of boreal fire emissions for North America in 2004: Importance of peat burning and pyroconvective injection, *J. Geophys. Res.*, 112, D12S03, doi:10.1029/2006JD007281, 2007.
- von Glasow, R., von Kuhlmann, R., Lawrence, M. G., Platt, U., and Crutzen, P. J.: Impact of reactive bromine chemistry in the troposphere, *Atmos. Chem. Phys.*, 4, 2481–2497, 2004, <http://www.atmos-chem-phys.net/4/2481/2004/>.
- Yokouchi, Y., Hasebe, F., Fujiwara, M., Takashima, H., Shiotani, M., Nishi, N., Kanaya, Y., Hashimoto, S., Fraser, P., Toom-Saunty, D., Mukai, H., and Nojiri, Y.: Correlations and emission ratios among bromoform, dibromochloromethane, and dibromomethane in the atmosphere, *J. Geophys. Res.*, 110, D23309, doi:10.1029/2005JD006303, 2005.
- Warwick, N. J., Pyle, J. A., Carver, G. D., Yang, X., Savage, N. H., O'Connor, F. M., and Cox, R. A.: Global modeling of biogenic bromocarbons, *J. Geophys. Res.*, 111, D24305, doi:10.1029/2006JD007264, 2006.
- Waugh, D. W., Strahan, S. E., and Newman, P. A.: Sensitivity of stratospheric inorganic chlorine to differences in transport, *Atmos. Chem. Phys.*, 7, 4935–4941, 2007, <http://www.atmos-chem-phys.net/7/4935/2007/>.
- WMO (World Meteorological Organization): *Scientific Assessment of Ozone Depletion: 2006*, Global Ozone Research and Monitoring Project – Report No. 50, Geneva, Switzerland, 2007.
- Yang, X., Cox, R. A., Warwick, N. J., Pyle, J. A., Carver, G. D., and O'Connor, F. M.: Tropospheric bromine chemistry and its impacts on ozone: A model study, *J. Geophys. Res.*, 110, D23311, doi:10.1029/2005-JD006244, 2005.